

Discrete-Time Analysis of Optimized Schwarz Waveform Relaxation Taking into Account Initial Robin Values on the Interface

Arthur Arnoult^[0009-0009-5077-9618],
Caroline Japhet^[0009-0000-1936-2106],
Pascal Omnes^[0000-0002-0480-7085]

1 Introduction

We consider the one-dimensional heat equation in $\Omega \times (0, T)$, with $\Omega = \mathbb{R}$ and final time $T > 0$,

$$\mathcal{L}u := \partial_t u - \nu \partial_{xx} u = f \quad \text{in } \Omega \times (0, T), \quad (1a)$$

$$u(\cdot, t = 0) = u_0 \quad \text{in } \Omega, \quad (1b)$$

$$\lim_{x \rightarrow \pm\infty} u(x, \cdot) \text{ is bounded on } (0, T), \quad (1c)$$

where f is a source term, u_0 an initial condition, and ν a positive diffusion coefficient.

Let us consider a decomposition of the domain Ω into two non-overlapping subdomains $\Omega_1 = (-\infty, 0)$ and $\Omega_2 = (0, +\infty)$. Note that the analysis presented in this article can be extended to the overlapping domain decomposition case. The OSWR method for solving (1) is an iterative method defined in Algorithm 1, involving Robin operators $\mathcal{B}_1 := \nu \partial_x + \alpha$ and $\mathcal{B}_2 := -\nu \partial_x + \alpha$, where $\alpha > 0$ is a coefficient chosen to accelerate convergence.

The usual analysis of the OSWR algorithm proves the convergence of the algorithm whatever the initialization of ξ_1^0, ξ_2^0 . Moreover, when it comes to choosing the Robin parameter, a Fourier analysis in time is used, and the parameter is defined as the one that optimizes the convergence for the "worst" Fourier mode.

This parameter is calculated in [4] as a function of the time step Δt , and gives (for all $\nu > 0$), $\alpha_C := \sqrt{\frac{\pi\nu}{\Delta t}} \left(\frac{\Delta t}{T}\right)^{1/4}$. This approach has met some success as reported in e.g. [4, 10, 5, 9] but we point here two improvements. First, since actual numerical

Arthur Arnoult · Caroline Japhet · Pascal Omnes

Université Sorbonne Paris Nord, LAGA, CNRS UMR 7539, Institut Galilée, 99 Av. J.-B. Clément,
93430 Villetaneuse, France, e-mail: arnoult@math.univ-paris13.fr, japhet@math.univ-paris13.fr

Pascal Omnes

Université Paris-Saclay, CEA, Service de Génie Logiciel pour la Simulation, 91191 Gif-sur-Yvette,
France, e-mail: pascal.omnes@cea.fr

Algorithm 1 (OSWR)

Choose initial Robin data ξ_1^0, ξ_2^0 on $(0, T)$ at $\{x = 0\}$, and set $\mathcal{B}_1 u_2^0(0, \cdot) := \xi_1^0$,
 $\mathcal{B}_2 u_1^0(0, \cdot) := \xi_2^0$.
for $\ell = 1, 2, \dots$ **do**
 Solve the local Robin problems
 $\mathcal{L}u_1^\ell = f|_{\Omega_1}$ in $\Omega_1 \times (0, T)$, $\mathcal{L}u_2^\ell = f|_{\Omega_2}$ in $\Omega_2 \times (0, T)$,
 $\mathcal{B}_1 u_1^\ell = \mathcal{B}_1 u_2^{\ell-1}$ on $\{x = 0\} \times (0, T)$, $\mathcal{B}_2 u_2^\ell = \mathcal{B}_2 u_1^{\ell-1}$ on $\{x = 0\} \times (0, T)$,
 $u_1^\ell(\cdot, 0) = u_0|_{\Omega_1}$ in Ω_1 , $u_2^\ell(\cdot, 0) = u_0|_{\Omega_2}$ in Ω_2 ,
 $\lim_{x \rightarrow -\infty} u_1^\ell(x, \cdot)$ is bounded, $\lim_{x \rightarrow +\infty} u_2^\ell(x, \cdot)$ is bounded.

end for

results that use Robin parameters obtained using Fourier transforms in time do not always perform as efficiently as expected [12, 6], other approaches, based on discrete-time analysis, were proposed in [3, 8, 2]. Secondly, in practical applications, when one uses the OSWR method on the whole time interval or on time windows (see e.g. [11, 12]) it is often usual to initialize the Robin data on the space-time interval (or window) by a constant in time function equal to the Robin operator \mathcal{B}_i applied to the initial condition, see for example [7] and [9, Section 6.2]. This is an appropriate choice, since it seems preferable to start as close as possible to the solution, and a good candidate for this is the solution at the initial time. In practice, we observe a significantly faster convergence than with random initial Robin data (that is traditionally used to illustrate the Fourier analysis), which we will verify in Section 4.

In this article, we aim to analyse the algorithm for such specific initial Robin data (i.e. by applying the Robin operator to a solution constant in time, equal to the initial condition). We do that by specializing the methodology of article [2] to initial Robin errors varying linearly in time.

We recall the analysis methodology and the main results of [2] in Section 2. In Section 3, we extend this analysis to the initialization of Robin quantities by the Robin operator \mathcal{B}_i applied to the initial condition, as discussed above. This makes it possible to define an optimized Robin parameter taking into account the initial Robin data, which, to our knowledge, has never been proposed before. Finally, in Section 4, we observe with various numerical cases that the parameter obtained is indeed an accurate approximation of the optimal parameter for different initial Robin data.

2 A reminder about discrete time analysis

For the analysis, we rely on the methodology of [2]. The idea is to introduce a time discretization with the backward Euler time scheme with N equal time steps Δt (the methodology and analysis can be extended to other time stepping schemes along the

same lines), to which we associate the sparse matrix A of size N , containing 1 on the diagonal and -1 on the sub-diagonal.

We can then write a discrete-time coupled problem associated with (1):
Find $U_1 \in (H^2(\Omega_1))^N$ and $U_2 \in (H^2(\Omega_2))^N$ such that

$$LU_1 = F_1 \quad \text{in } \Omega_1, \quad LU_2 = F_2 \quad \text{in } \Omega_2, \quad (2a)$$

$$B_1U_1 = B_1U_2 \quad \text{at } \{x = 0\}, \quad B_2U_2 = B_2U_1 \quad \text{at } \{x = 0\}, \quad (2b)$$

$$\lim_{x \rightarrow -\infty} U_1(x) \quad \text{is bounded}, \quad \lim_{x \rightarrow +\infty} U_2(x) \quad \text{is bounded}, \quad (2c)$$

with, the following definitions for $i = 1, 2$:

- discrete heat operator $L := \frac{1}{v\Delta t}A - \partial_{xx}$;
- discrete source term $F_i := (F_{i,1}, \dots, F_{i,N})^T$, with $F_{i,n}(x) := \frac{f(x,n\Delta t)|_{\Omega_i}}{v} + \frac{u_0(x)|_{\Omega_i}}{v\Delta t} \delta_{1n}$, (where δ_{1n} is the Kronecker delta);
- discrete Robin operator B_i being the extension of \mathcal{B}_i to vectors of $(H^2(\Omega_i))^N$.

Then, Algorithm 2 is a discrete-time version of Algorithm 1 that solves (2).

Algorithm 2 (Discrete-time OSWR)

Choose initial Robin data $\Xi_1^0, \Xi_2^0 \in \mathbb{R}^N$ at $\{x = 0\}$, and set $B_1U_2^0 := \Xi_1^0, B_2U_1^0 := \Xi_2^0$.

for $\ell = 1, 2, \dots$ **do**

Solve the local Robin problems

$$LU_1^\ell = F_1 \quad \text{in } \Omega_1, \quad LU_2^\ell = F_2 \quad \text{in } \Omega_2,$$

$$B_1U_1^\ell = B_1U_2^{\ell-1} \quad \text{at } \{x = 0\}, \quad B_2U_2^\ell = B_2U_1^{\ell-1} \quad \text{at } \{x = 0\},$$

$$\lim_{x \rightarrow -\infty} U_1^\ell(x) \quad \text{is bounded}, \quad \lim_{x \rightarrow +\infty} U_2^\ell(x) \quad \text{is bounded}.$$

end for

We wish to analyse the convergence of Algorithm 2. We first introduce the following notations: $\bar{\alpha} := \sqrt{\frac{\Delta t}{v}}\alpha$ and, for each subdomain Ω_i , for $i = 1, 2$:

- exact solution in subdomain: $u_i := u|_{\Omega_i}$;
- initial condition in subdomain: $u_{0,i} := u_0|_{\Omega_i}$;
- OSWR interface error: $\beta_i^\ell := U_i^\ell(0) - U_i(0)$.

We recall here the main convergence theorem, obtained in [2].

Theorem 1 (OSWR convergence) *Let $u_0 \in H^1(\Omega)$, $f \in L^2(0, T; L^2(\Omega))$, $\alpha > 0$. Then, Alg. 2 converges in $((H^1(\Omega_1))^N \cap (L^\infty(\Omega_1))^N) \times ((H^1(\Omega_2))^N \cap (L^\infty(\Omega_2))^N)$ to the solution (U_1, U_2) of (2).*

Furthermore, the relation between the first interface error vector and the initial dimensionless discrete Robin error on the interface is given, for all $i = 1, 2$, by (see [2, Equation (26a)])

$$\beta_i^1 = (\bar{\alpha}\mathbf{I}_N + \sqrt{A})^{-1}\bar{G}_i^0, \quad (3)$$

where \mathbf{I}_N denotes the identity matrix of size N , \sqrt{A} denotes the matrix whose square is A and with positive eigenvalues, and

$$\bar{G}_i^0 := \sqrt{\Delta t/\nu}(\Xi_i^0 - (B_i U_i)(0)). \quad (4)$$

Moreover, setting

$$M(\bar{\alpha}) := \left((\bar{\alpha} \mathbf{I}_N + \sqrt{A})^{-1} (\bar{\alpha} \mathbf{I}_N - \sqrt{A}) \right)^2,$$

the discrete-time interface errors are given, for all $\ell \in \mathbb{N}$, by

$$\beta_i^{2\ell+1} = (M(\bar{\alpha}))^\ell \beta_i^1. \quad (5)$$

Relation (5) tells us that the convergence is driven by matrix M and thus, for a given N , the convergence depends only on $\bar{\alpha}$ and \bar{G}_i^0 , and in [2] we defined $\bar{\alpha}_{D[2\ell+1]} := \operatorname{argmin}_{\bar{\alpha} \in]0,1[} \|M^\ell(\bar{\alpha})\|_\infty$. But we also deduce that the initial error β_i^1 weights the coefficients of this matrix. In an effort to estimate this influence, from (3) we need to focus on the initial error \bar{G}_i^0 , which can be done assuming a shape for this error. This is the aim of the next part.

3 Taking into account the OSWR initialization

We now consider the case where Algorithm 1 is initialized, on $(0, T)$, with,

$$\xi_i^0 = \mathcal{B}_i(u_{0,i})(x=0), \quad i = 1, 2,$$

which is well defined if $u_{0,i} \in H^2(\Omega_i)$. Similarly, if $U_{0,i} \in (H^2(\Omega_i))^N$ is the vector of size N where all components are $u_{0,i}$, we choose in Algorithm 2,

$$\Xi_i^0 = B_i(U_{0,i})(x=0). \quad (6)$$

We introduce here a discrete time analysis taking into account the choice (6), from which we will deduce optimized Robin parameters.

Theorem 2 *Let $\ell \geq 0$, $i = 1, 2$. Suppose that the solutions of (2) verify*

$$(U_i)_n \underset{T \rightarrow 0}{=} u_i(\cdot, n\Delta t) + \mathcal{O}(T\Delta t), \quad \text{for all } n \in \{1, \dots, N\}. \quad (7)$$

Let us define the vector $K_\ell(\bar{\alpha}) := (M(\bar{\alpha}))^\ell (\bar{\alpha} \mathbf{I}_N + \sqrt{A})^{-1} (1, 2, \dots, N)^T$.

If the initial Robin data are chosen with (6), and if the exact solution u is of class $\mathcal{C}^2([0, T])$ on the interface, then there exist real constants (C_1, C_2) such that the error vector on the interface verifies, for small T ,

$$\beta_i^{2\ell+1} \underset{T \rightarrow 0}{=} C_i K_\ell(\bar{\alpha}) + \mathcal{O}(T^2), \quad \text{and} \quad \|\beta_i^{2\ell+1}\|_\infty \underset{T \rightarrow 0}{=} |C_i| \|K_\ell(\bar{\alpha})\|_\infty + \mathcal{O}(T^2). \quad (8)$$

Proof. Let $\ell \geq 0$ and $i = 1, 2$. From formulas (5) and (3), we need to estimate \bar{G}_i^0 in order to evaluate $\beta_i^{2\ell+1}$. For this, we start from (4) and from the choice (6) and obtain, applying (7), for all $n \in \{1, \dots, N\}$:

$$\begin{aligned} (\bar{G}_i^0)_n &= \sqrt{\Delta t/\nu} (B_i(U_{0,i})_n - B_i(U_i)_n)(x=0) \\ &= \sqrt{\Delta t/\nu} (\mathcal{B}_i(u_{0,i}) - \mathcal{B}_i(u_i(\cdot, n\Delta t)))(x=0) + \mathcal{O}(T\Delta t), \end{aligned}$$

as $T \rightarrow 0$. The sequel of the proof is based on a Taylor expansion around the initial time. For short times T , there exists a function (of space) D_i such that the solution of problem (1) is written in Ω_i ,

$$u_i(x, t) \underset{T \rightarrow 0}{=} u_i(x, 0) + D_i(x)t + \mathcal{O}(T^2) \quad \text{on } (0, T).$$

Thus, we obtain,

$$(\mathcal{B}_i(u_{0,i}) - \mathcal{B}_i(u_i(\cdot, n\Delta t)))(x=0) = -(\mathcal{B}_i(D_i))(x=0) n\Delta t + \mathcal{O}(T^2),$$

which leads to

$$\bar{G}_i^0 \underset{T \rightarrow 0}{=} \Delta t \left((-1)^{i+1} \sqrt{\Delta t \nu} \partial_x + \bar{\alpha} \right) (D_i)(x=0) (1, 2, \dots, N)^T + \mathcal{O}(T^2),$$

as $\mathcal{O}(T\Delta t)$ is dominated by $\mathcal{O}(T^2)$. Then, from formulas (5) and (3), we get (8) with $C_i := \Delta t \left((-1)^{i+1} \sqrt{\Delta t \nu} \partial_x + \bar{\alpha} \right) (D_i)(x=0)$, which shows that the convergence depends on $\bar{\alpha}$ and only weakly on ν , at least for small $\sqrt{\Delta t \nu}$. \square

We now have an estimate of the error at the interface. To minimize the algorithm error, we define the optimized Robin parameter as follows:

$$\bar{\alpha}_{I[\ell]} := \operatorname{argmin}_{\bar{\alpha} \in]0,1]} \|K_\ell(\bar{\alpha})\|_\infty. \quad (9)$$

This parameter is then calculated using the methodology described in [2, Section 4.5], with a similar calculation cost.

From equation (8), one can construct an abacus by plotting $\|K_{\frac{\ell-1}{2}}(\bar{\alpha}_{I[\ell]})\|_\infty$ as a function of ℓ , in the spirit of [2, Section 5.3.2]. This allows to recommend a couple (number of iterations, Robin parameter) to reach a given relative accuracy (e.g. the expected accuracy of the numerical scheme).

4 Numerical results

We consider $\Omega = [-1/2, 1/2]$, uniformly meshed with mesh size $\Delta x = 10^{-3}$. Final time is $T = 1$ or $T = 5$, and time steps are $\Delta t = T/N$, with $N = 100$ (similar results are obtained with other values of N , see [1, Section 7.1.2]). We use a finite element discretization in space, and a backward Euler scheme in time. We

consider a diffusion coefficient $\nu = 0.05$. For domain decomposition, the interface is placed at $\{x = 0\}$. For this study, we consider two different cases of regular exact solutions $u(x, t)$, which defines the initial condition $u_0(x, t) = u(x, 0)$ and the source term $f(x, t) = (\partial_t - \nu \partial_{xx})u(x, t)$. The OSWR algorithm is then initialized with constant in time Robin data, defined by $\xi_i^0 = \mathcal{B}_i(u_{0,i})$, for $i = 1, 2$.

We want to verify that the shape of $\bar{\alpha} \mapsto \|K_\ell(\bar{\alpha})\|_\infty$, in the interface error (8), gives a good estimate of the shape of the actual numerical error, and therefore that the discrete optimized parameter (9) is a close estimate of the optimal one. To do this, we plot the ratios of the $L^\infty(]0, T[)$ -norm of the errors on the interface between the discrete monodomain solution and the OSWR-solution at a given iteration ℓ , over the $L^\infty(]0, T[)$ -norm on the interface of the discrete monodomain solution, versus $\bar{\alpha}$, for solutions depending on time like sine and cosine. We consider two different convergence regimes (see [2]): iteration $\ell = 7$ (superlinear) and $\ell = 21$ (linear).

We overlay the curve $\bar{\alpha} \mapsto \|K_\ell(\bar{\alpha})\|_\infty/N$ (the scaling by N is for readability only, as the bound is up to a constant; with the log-scale, this will not change the shape of the curve, and thus the value of the optimal parameter) since this is the bound that we actually minimize. We also superimpose the error curve obtained with a zero initial condition and source term, starting from Robin quantity $g_i^0(t) = t$. Indeed, it is this error that we study in this analysis as a proxy for the actual error.

The triangles indicate the discrete-time optimized parameters $\bar{\alpha}_{I[\cdot]}$ defined in (9), the squares are for $\bar{\alpha}_{D[\cdot]}$ (defined page 4) and the stars stand for $\bar{\alpha}_C = (\Delta t/\nu)^{1/2} \alpha_C$. We obtain $\bar{\alpha}_C = 0.56$, $\bar{\alpha}_{I[7]} = 0.27$, $\bar{\alpha}_{I[21]} = 0.53$, $\bar{\alpha}_{D[7]} = 0.40$ and $\bar{\alpha}_{D[21]} = 0.56$.

Sine in time

First, we can see from Figure 1 that convergence can be much faster starting from a Robin data calculated from the initial condition than for randomly chosen data, especially at iteration 7. It therefore seems appropriate to start with Robin data calculated from the initial condition, and to choose a suitable Robin parameter, which is significantly different from the one obtained with the random initialization. We observe on Figure 2 that estimate (8) is really close to the real curve versus $\bar{\alpha}$,

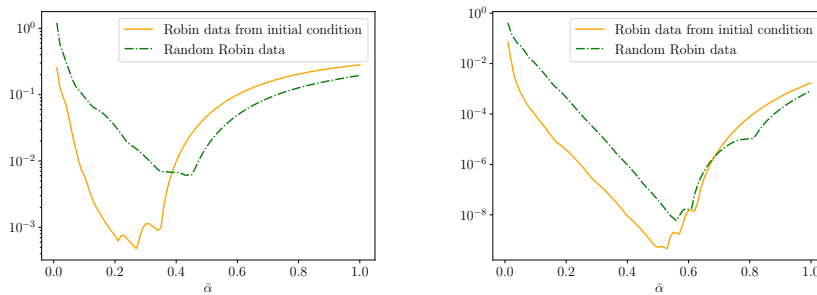


Fig. 1 Comparison of the relative $L^\infty(]0, T[)$ -error on the interface, versus $\bar{\alpha}$, starting from a Robin data calculated with initial condition or with random values, at iterations 7 (left) and 21 (right), with $N = 100$, for $T = 1$, for the exact solution $u(x, t) = \sin(\pi t)(\sin(\pi x) + \cos(\pi x))$.

which shows that this relation is a good estimation of the error obtained in practice. The optimized parameter $\bar{\alpha}_{I[\cdot]}$ gives a good approximation of the numerical optimal parameter, and a better one than $\bar{\alpha}_{D[\cdot]}$ and $\bar{\alpha}_C$, especially at iteration 7, where the error is about 10 (resp. 100) times smaller compared to $\bar{\alpha}_{D[7]}$ (resp. $\bar{\alpha}_C$).

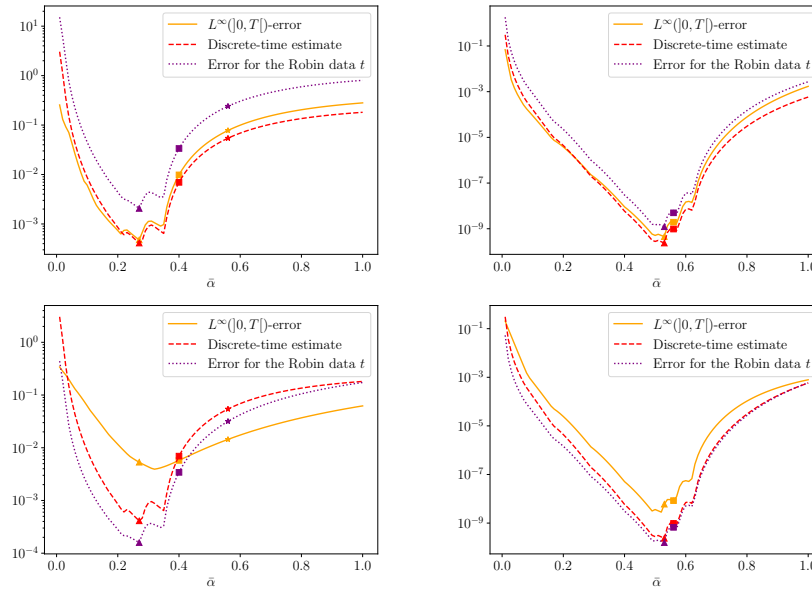


Fig. 2 Relative $L^\infty(]0, T[)$ -error versus $\bar{\alpha}$ at iterations 7 (left) and 21 (right), for $N = 100$, with $T = 1$ (up) and $T = 5$ (down), for the exact solution $u(x, t) = \sin(\pi t)(\sin(\pi x) + \cos(\pi x))$.

In the proof of Theorem 2, we assume that the time dependence of the exact solution is of the form $u_0 + Ct$. This Taylor expansion is reasonable for short times, but it appears from Figure 2 that even for large final times ($T = 5$), the results we obtain are also satisfying. Similar satisfactory results were observed in [1, Section 7.1.2.2] with the exact solution $1 + t + t^2$ in time, with final time $T = 1$, mimicking a situation in which higher order terms in the Taylor expansion are not negligible on the whole time interval. Although these situations are outside the range of the theorem, and the estimate is probably not as accurate as for short final times, the parameter obtained with (9) remains a very good choice, even if the final time T is large.

Cosine in time

With the exact solution taken in the form of a sine in time, we indeed had, for short times, an exact solution of the form $u_0 + Ct$. But what if the exact solution has no term of order 1, as with a cosine in time? We observe again on Figure 3 that the discrete optimized parameter is still close to the numerical optimal parameter.

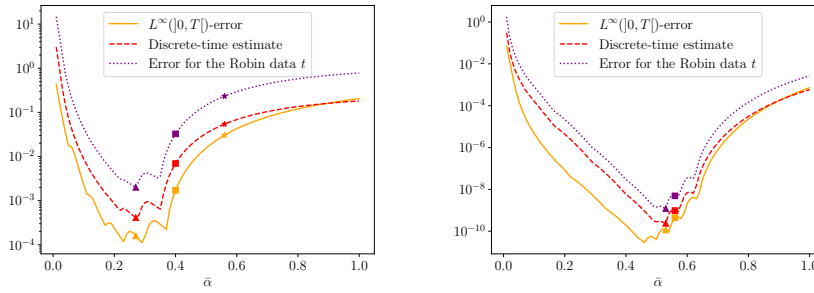


Fig. 3 Relative $L^\infty([0, T])$ -error versus $\bar{\alpha}$ at iterations 7 (left) and 21 (right), with $N = 100$, for $T = 1$, for the exact solution $u(x, t) = \cos(\pi t)(\sin(\pi x) + \cos(\pi x))$.

References

1. Arnault, A.: Méthode de décomposition de domaine espace-temps et parallèle en temps pour les écoulements incompressibles et nouvelle analyse de la méthode de relaxation d'onde de Schwarz optimisée. PhD Thesis, Université Sorbonne Paris-Nord - Paris XIII (2025). URL <https://theses.hal.science/tel-05419636>
2. Arnault, A., Japhet, C., Omnes, P.: Discrete-time analysis of optimized Schwarz waveform relaxation with Robin parameters depending on the targeted iteration count. *ESAIM: Math. Model. Numer. Anal.* **57**(4), 2371–2396 (2023)
3. Clement, S., Lemarié, F., Blayo, E.: Discrete analysis of Schwarz waveform relaxation for a diffusion reaction problem with discontinuous coefficients. *SMAI J. Comput. Math.* **8**, 99–124 (2022)
4. Gander, M.J., Halpern, L.: Méthodes de relaxation d'ondes (SWR) pour l'équation de la chaleur en dimension 1. (Optimized Schwarz waveform relaxation (SWR) for the one-dimensional heat equation). *C. R., Math., Acad. Sci. Paris* **336**(6), 519–524 (2003)
5. Gander, M.J., Halpern, L.: Optimized Schwarz waveform relaxation methods for advection reaction diffusion problems. *SIAM J. Numer. Anal.* **45**(2), 666–697 (2007)
6. Gander, M.J., Martin, V.: Why Fourier mode analysis in time is different when studying Schwarz Waveform Relaxation. *J. Comput. Phys.* **491**, 112316 (2023). Publisher: Elsevier
7. Halpern, L., Japhet, C., Szeftel, J.: Optimized Schwarz waveform relaxation and discontinuous Galerkin time stepping for heterogeneous problems. *SIAM J. Numer. Anal.* **50**(5), 2588–2611 (2012)
8. Haynes, R.D., Mohammad, K.: Fully discrete Schwarz waveform relaxation analysis for the heat equation on a finite spatial domain. *ESAIM: Math. Model. Numer. Anal.* **57**(4), 2397–2426 (2023)
9. Hoang, T.T.P., Jaffré, J., Japhet, C., Kern, M., Roberts, J.E.: Space-time domain decomposition methods for diffusion problems in mixed formulations. *SIAM J. Numer. Anal.* **51**(6), 3532–3559 (2013)
10. Martin, V.: An optimized Schwarz waveform relaxation method for the unsteady convection diffusion equation in two dimensions. *Appl. Numer. Math.* **52**(4), 401–428 (2005)
11. Martin, V.: Schwarz waveform relaxation algorithms for the linear viscous equatorial shallow water equations. *SIAM J. Sci. Comput.* **31**, 3595–3625 (2009)
12. Thery, S., Pelletier, C., Lemarié, F., Blayo, E.: Analysis of Schwarz Waveform Relaxation for the Coupled Ekman Boundary Layer Problem with Continuously Variable Coefficients. *Numer. Algorithms.* **89**, 1145–1181 (2022)